

Enhancing Load Range Of Concurrent Dual-Band Complex To Real Matching Networks Using Load Shifters

Shadab Rabbani^{1*}, Umar Farooque², Faiz Ahmad³, Rakesh Kumar⁴

^{1*,2,3,4}Muzaffarpur Institute of Technology, Muzaffarpur, India. *Email: shadab.ece@mitmuzaffarpur.org

Citation: Shadab Rabbani, et al (2023), Enhancing Load Range Of Concurrent Dual-Band Complex To Real Matching Networks Using Load Shifters, *Educational Administration: Theory and Practice*, 29(4)1, 2565 - 2571
Doi: 10.53555/kuey.v29i4.7227

ARTICLE INFO

ABSTRACT

This paper presents enhancement of the load range of dual band matching networks (DBMNs) for complex to real (C2R) impedance matching through load shifters. The proposed load shifter is a simple structure and has versatility to serve any impedance environment for any frequency ratio. In this paper, the limitations of a single section transmission line used for transforming frequency dependent complex loads (FDCLs) to complex conjugate loads (CCLs) in many earlier reported DBMNs has been discussed. The possible range of loads at one frequency if the load at other frequency is given is thoroughly studied. A load shifting approach for shifting the loads to the values such that FDCLs can be transformed to CCLs is proposed. Two prototype MNs with frequency ratios 1.6 and 5.6 respectively wherein the proposed load shifters are successfully applied are designed, simulated and fabricated. The simulated and the measured results are in a good accordance. This scheme can also be used with any other regular DBMN having load constraints.

Keywords: Dual-band, matching network, Transmission line, Complex to real impedance matching.

1. INTRODUCTION

The impedance transformer, also known as the impedance matching network, is a ubiquitous component in microwave systems. Their primary purpose is to lessen reflections between two circuits or related components [1]. In 2003, Monzon presented a two-stage stepped impedance transmission line structure for real- to-real (R2R) impedance matching [2]. These MNs are utilized in power dividers, couplers and other applications where two real impedances need to be matched at two frequencies. Sometimes, they are also used in C2R impedance matching, when FDCLs are first transformed to real loads from where impedance transformation is done through R2R impedance transformer [3]. The Monzon's structure can be used only for a limited load range for a given frequency ratio. The limitations of such structures along with load shifting techniques to enhance their load range has been discussed in [4].

A lot of dual-band (DB) matching schemes for C2R impedance matching has been reported so far. Some of the schemes transform the FDCLs to CCLs using a single section transmission line as the first stage [3], [5]–[12]. MNs with this transmission line can be used only for limited load combinations. This limitation has been overcome in [13] by using topologies where in such transmission line is not used. In [14], a load healing concept has been used to convert the loads through load healers such that the new FDCLs can be transformed to CCLs through the transmission line. The load healers used can be a series transmission line, a stub or a combination of the two. Though the scheme works well, but the approach is completely based on iterations and hit and trial methods.

In this paper, the limitations of transforming FDCLs to CCLs has been discussed. Also, the possible range of loads for one frequency if the load at second frequency is given is studied. A load shifting approach for shifting the loads to the values such that FDCLs can be transformed to CCLs is proposed. Unlike [14], the transformation of loads by transmission line has been studied on Smith chart and load shifters for different cases are designed accordingly. The load shifter is a single series transmission line. The characteristic impedance and electrical length of this transmission line can be changed to obtain multiple solutions. Two prototype MNs wherein the proposed load shifters are successfully applied are designed, simulated and fabricated. The simulated and the measured results are in a good accordance. This scheme can also be used with any other regular DBMN having load constraints.

2. SINGLE SECTION TRANSMISSION LINE AS FDCL TO CCL TRANSFORMER

A single section transmission line for FDCL to CCL transformation is given in Fig. 1. The mathematical equations for Z_T and θ_T can be obtained from [3], [5] – [12]:

$$Z_T = \sqrt{(R_1 R_2 + X_1 X_2) - \frac{R_2 X_1 - R_1 X_2}{R_2 - R_1} (X_1 + X_2)} \quad (1)$$

$$\theta_T = \frac{p\pi + \tan^{-1}\left(\frac{Z_1(R_1 - R_2)}{R_2 X_1 - R_1 X_2}\right)}{m+1}; \quad p \in Z \quad (2)$$

where $m = f_2/f_1$ is the frequency ratio.

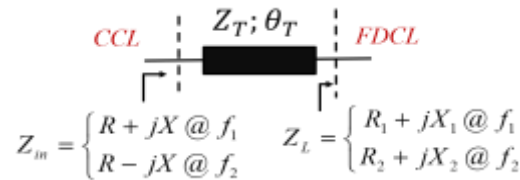


Fig. 1. Single section transmission line for FDCL to CCL transformation.

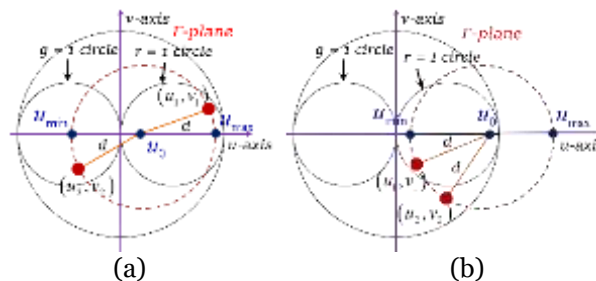


Fig. 2. Representation of impedance transformation for transmission line on Smith chart when FDCL to CCL transformation is (a) feasible (b) not feasible

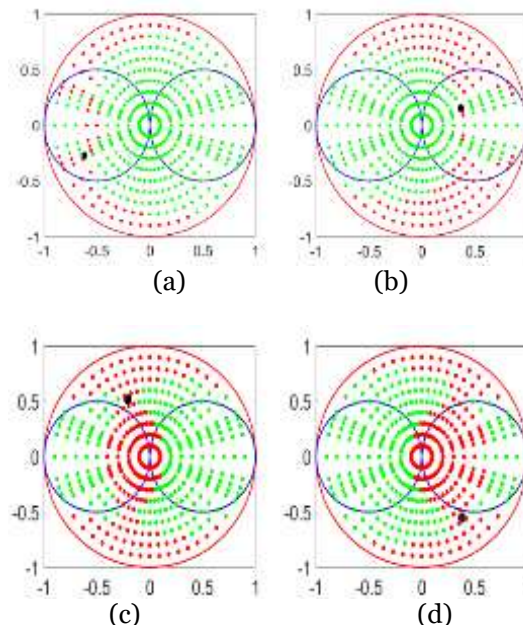


Fig. 3. Possible loads at f_2 if Z_{L1} is (a) inside $g = 1$ circle, (b) inside $r = 1$ circle, (c) inductive load outside both $g = 1$ and $r = 1$ circles, and (d) capacitive load outside both $g = 1$ and $r = 1$ circles.

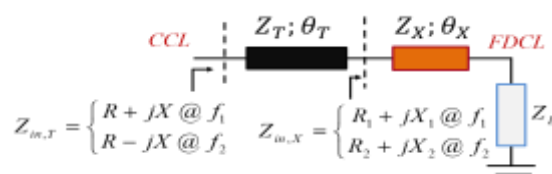


Fig. 4. Shifting of loads using load shifter.

The characteristic impedance of the transmission line for FDCL to CCL transformation does not depend upon the frequency ratio, but depends only upon the load values (1). Though they do not have any frequency constraints, but they can be used only under certain load conditions. Their limitations are discussed in details in [13]. However, a different perspective for their limitations using Smith chart is discussed in the subsequent subsection.

2.1 Understanding limitations of single section transmission line as FDCL to CCL transformer:

Smith chart is a unity circle representing Γ -plane, where $\Gamma = u + jv = (Z_L - 1)/(Z_L + 1)$. In Fig. 2, the coordinates (u_1, v_1) and (u_2, v_2) represent loads Z_{L1} and Z_{L2} respectively. A transmission line moves a load on a circle. A circle is referred to as a constant VSWR circle if the transmission line's characteristic impedance is $Z_T = Z_0$ and its center is located at the Smith chart's center. However, if $Z_T \neq Z_0$, then the centre of the circle lies at a point on the real axis other than the origin [15]. The loads are moved to two symmetrically opposite points along the real axis to transform to two complex conjugate impedances/admittances. This means that the two load points must sit on the same circle due to the transmission line's characteristic impedance, Z_T . In Fig. 2, u_0 is the centre of that circle. u_{min} and u_{max} are the minimum and maximum values through which the circle passes through the u-axis, and 'd' is the radius of the circle. Then,

$$u_0 = \frac{1}{2} \frac{(v_2^2 - v_1^2) + (u_2^2 - u_1^2)}{u_2 - u_1} \quad (3)$$

FDCLs can be transformed to CCLs through a single transmission line only if all the points of the corresponding circle lie inside the unity circle, which means $u_{min} = (u_0 - d) > -1$ and $u_{max} = (u_0 + d) < 1$. This puts up a very stringent requisition and therefore such structures can be used only for a limited number of load combinations. Fig. 2 shows the movement of two loads on the circle corresponding to the single section transmission line. Fig. 2(a) shows the load positions when the transmission line can transform FDCLs to CCLs and Fig. 2(b) shows the condition when u_{max} is lying outside the unity circle and hence the transformation is not possible.

2.2 Range of Z_{L2} for which FDCL to CCL transformation is feasible for a given Z_{L1} :

Fig.3 shows the possible loads at second frequency if the load at first frequency is given. The black dots represent Z_{L1} , the green dots represent possible values of Z_{L2} and the red dots represent the values for which the transformation is not feasible. Fig.3(a) shows the case if Z_{L1} is inside $g = 1$ circle, (b) inside $r = 1$ circle, (c) inductive load outside both $g = 1$ and $r = 1$ circles and (d) capacitive load outside both $g = 1$ and $r = 1$ circles respectively. From Fig. 3(a), it can be observed that if Z_{L1} is lying inside $g = 1$ circle, then almost all the load points inside $r = 1$ circle can be possible values for Z_{L2} . Similarly, from fig.3(b), if Z_{L1} is lying inside $r = 1$ circle, then almost all the load points inside $g = 1$ circle can be possible values for Z_{L2} . Also fig.3(c)-(d) suggest that if the two loads lie in two opposite sides, i.e.

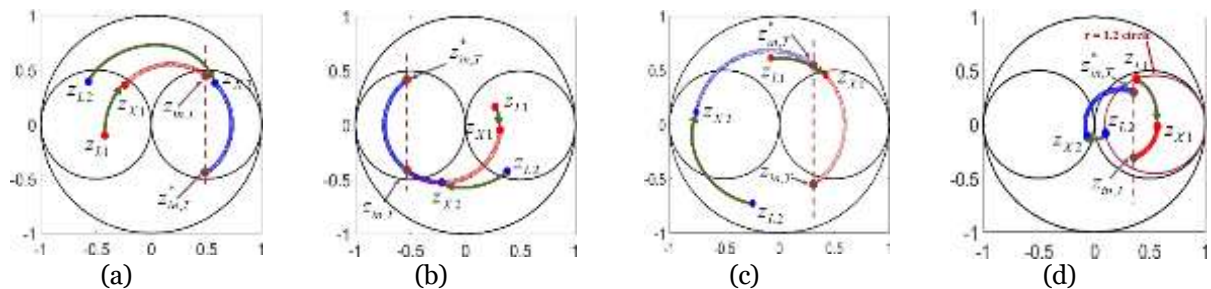


Fig.5. Load transformation at $f_1=1\text{GHz}$ and $f_2=1.6\text{GHz}$ for (a)case-a, (b)case-b, (c)case-c, and (d)case-d

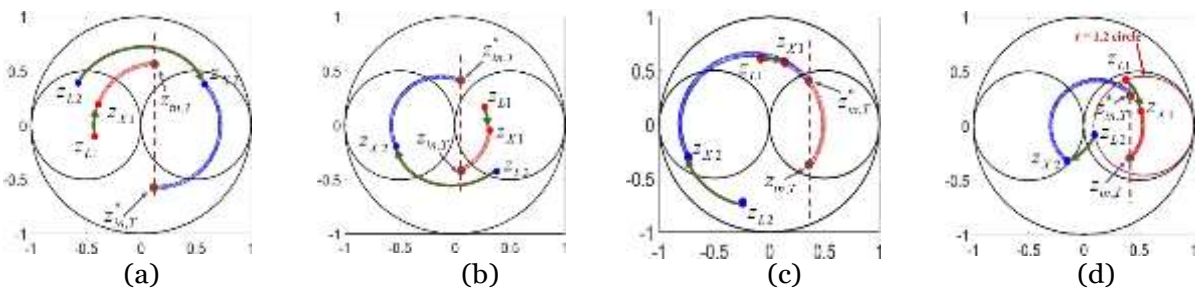


Fig.6. Load transformation at $f_1=1\text{GHz}$ and $f_2=2.8\text{GHz}$ for (a)case-a, (b)case-b, (c)case-c, and (d)case-d

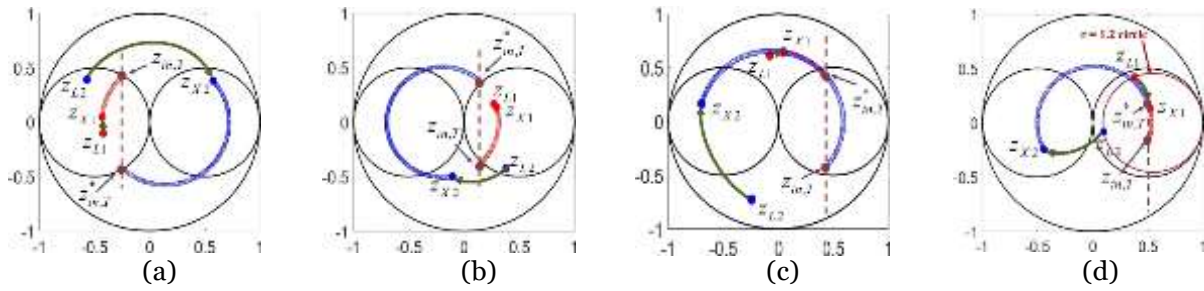


Fig.7. Load transformation at $f_1=1\text{GHz}$ and $f_2=5.6\text{GHz}$ for (a)case-a, (b)case-b, (c)case-c, and (d)case-d

one in the left and other in the right half planes of Smith chart, then it is likely that they form a set of possible values.

2.3 Load Shifter for enhancing the load range:

As shown in fig. 4, FDCLs which can't be transformed to CCLs can be shifted through load shifters such that the modified loads can be transformed. From fig.3, the best chances for feasibility of FDCL to CCL transformation is when one of the loads lies inside $g=1$ circle and the other inside $r=1$ circle. If not, the none lies in the left half plane and the other in the right half. Fig.5, fig.6 and fig.7 shows how an otherwise infeasible load combination can be made feasible with the help of load shifters at frequency ratios 1.6, 2.8 and 5.6 respectively for the following four different cases.

Case-1: Both Z_{L1} and Z_{L2} lying inside $g=1$ circle.

Case-2: Both Z_{L1} and Z_{L2} lying inside $r=1$ circle.

Case-3: Both Z_{L1} and Z_{L2} lying outside $r=1$ and $g=1$ circles.

Case-4: Both Z_{L1} and Z_{L2} lying on same r -circle.

Table-I shows the values of Z_X , θ_X , Z_T , θ_T , $Z_{in,X}$ and $Z_{in,T}$ for each case for all the three frequency conditions.

3. DESIGN OF DUAL BAND MATCHING NETWORK (DBMN) USING LOAD SHIFTER

The DBMN is shown in fig. 8. $Y_{in,T}$ is complex conjugate admittance at the two frequencies. The complex conjugate susceptances are cancelled by the open/short stub. If the susceptances are difficult to be cancelled through a single stub, then double stub or branched stub structures can also be used. The left behind real load is then matched through Monzon's structure [2]. The design steps and two design examples are presented in the next subsections. The prototype DBMNs are designed at frequency ratio, $m=1.6$ and 5.6 respectively. The frequencies are chosen such that the proposed scheme can be validated at both low as well as high frequency ratios.

TABLE I. Z_X , θ_X , Z_T , θ_T , $Z_{in,X}$ and $Z_{in,T}$ for different cases.

Case	$m=f_2/f_1$	Z_T (Ω)	Z_X (Ω); θ_X (deg)	Z_T (Ω); θ_T (deg) after load shifting	$Z_{in,X}$ (Ω)		$Z_{in,T}$ (Ω)	
					at f_1	at f_2	at f_1	at f_2
case(a) $Z_{L1}=20-j5$ $Z_{L2}=10+j15$	1.6	j15	50;35	85.2;39.6	24.4+j21.7	80.7+j117	60.5+j98.7	60.5-j98.7
	2.8		50;20	79.3;28.7	20.7+j9.8	80.7+j117	30.2+j52.4	30.2-j52.4
	5.6		50;10	78;17.3	19.8+j2.4	80.7+j117	22+j25.2	22-j25.2
case(b) $Z_{L1}=80+j30$ $Z_{L2}=60-j75$	1.6	j122.5	50;20	27.1;54.8	95.4-j9.4	19.3-j30.1	10.5-j15.9	10.5+j15.9
	2.8		50;20	35.9;26.9	95.4-j9.4	14.2-j8.1	38.6-j38.2	38.6+j38.2
	5.6		60;5	29.1;23.3	86.9+j26.3	25.2-j33.9	51-j43.4	51+j43.4
case(c) $Z_{L1}=20+j40$ $Z_{L2}=10-j35$	1.6	j25.5	50;25	36.1;38.9	56.9+j84.1	6.7+j3.7	39.6-j72.1	39.6+j72.1
	2.8		40;10	27.7;34.9	30.1+j53.9	5.9-j9.9	64-j70	64+j70
	5.6		80;5	40;17.8	22+j48.6	8.4+j5.7	60.5+j83.4	60.5-j83.4
case(d) $Z_{L1}=60+j75$ $Z_{L2}=60-j10$	1.6	Inf	50;25	87.7;37	181-j10	43-j9.7	78.8-j61.3	78.8+j61.3
	2.8		30;10	67;32.4	141+j54.3	30.6-j22.6	97.7-j70.2	97.7+j70.2
	5.6		30;10	52.2;16.9	141+j54.3	17.4-j11.5	135-j59.9	135+j59.9

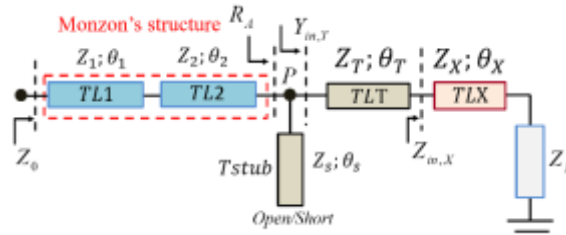


Fig.8. Dual band matching network.

3.1 Design steps:

Step-1: Calculate Z_T and θ_T using (1) and (2).

Step-2: If Z_T is realizable, skip load shifter as of now. If not, plot Z_{L1} and Z_{L2} on a Smith chart and estimate the values of θ_X such that load at one frequency can be shifted inside or close to $g=1$ circle and the other to $r=1$ circle. Calculate $Z_{in,X}$ as follows:

$$Z_{in,X}|_{f1} = Z_X \left(\frac{Z_{L1} + jZ_X \tan(\theta_X)}{Z_X + jZ_{L1} \tan(\theta_X)} \right) \quad (4)$$

And

$$Z_{in,X}|_{f2} = Z_X \left(\frac{Z_{L2} + jZ_X \tan(m\theta_X)}{Z_X + jZ_{L2} \tan(m\theta_X)} \right) \quad (5)$$

Step-3: Calculate Z_T and θ_T . If Z_T is realizable, move to next step, else modify the values of Z_X and/or θ_X .

Step-4: Calculate $Y_{in,T}$ as follows:

$$Y_{in,T}|_{f1} = \frac{1}{Z_T} \left(\frac{Z_T + jZ_{in,X}|_{f1} \tan(\theta_X)}{Z_{in,X}|_{f1} + jZ_T \tan(\theta_X)} \right) \quad (6)$$

And

$$Y_{in,T}|_{f2} = \frac{1}{Z_T} \left(\frac{Z_T + jZ_{in,X}|_{f2} \tan(m\theta_X)}{Z_{in,X}|_{f2} + jZ_T \tan(m\theta_X)} \right) \quad (7)$$

Step-5: The susceptances of $Y_{in,T}|_{f1}$ and $Y_{in,T}|_{f2}$ are complex conjugates. Design the stub for susceptance cancellation.

Step-6: Calculate R_A as follows:

$$R_A = \frac{1}{\text{Re}(Y_{in,T}|_{f1})} = \frac{1}{\text{Re}(Y_{in,T}|_{f2})} \quad (8)$$

Step-7: Check for the feasibility of realization of R_A for the given frequency ratio using Monzon's structure as given in [4]. If R_A is realizable, design the Monzon's structure as given in [2]. Else modify Z_X and/or θ_X .

3.2 Design example-1: DBMN at $m = 1.6$

($f_1=1\text{GHz}$, $f_2=1.6\text{GHz}$, $Z_{L1}=10-j41.95\Omega$ and $Z_{L2}=10-j8.82\Omega$). Since the two loads lie on the same r -circle, Z_T as calculated from (1) is infinity. The loads are implemented using a 10Ω SMD resistor followed by an open stub of $W=1.15\text{mm}$ and $L=12.95\text{mm}$. This open stub gives an electrical length of 50° at 1GHz .

3.3 Design example-2: DBMN at $m = 5.6$

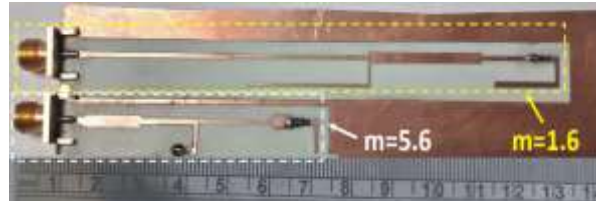
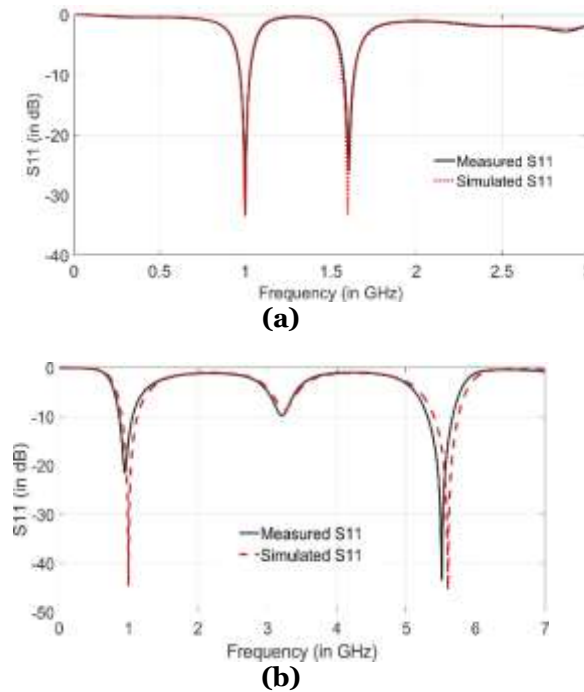
($f_1=1\text{GHz}$, $f_2=5.6\text{GHz}$, $Z_{L1}=100-j137.37\Omega$ and $Z_{L2}=100+j20.2\Omega$). Like example-1, since the two loads lie on the same r -circle, Z_T is infinity. The loads are implemented using a 100Ω SMD resistor followed by an open stub of $W=1.15\text{mm}$ and $L=10.23\text{mm}$. This open stub gives an electrical length of 20° at 1GHz .

3.4 Prototyping and measurement:

Changing the values of Z_X and θ_X give multiple design options. The favorable ones are fabricated on ROGERS RO4003 substrate ($\epsilon_r=3.28$, height = 20 mils, copper cladding thickness= $35\mu\text{m}$). The fabricated structures are given in Fig.9. The structures are simulated using Keysight ADS design tool. The reflection coefficient for the fabricated structure is measured on VNA. The optimized design dimensions (in mm) are given in Table II. The Electromagnetic (EM) simulated and measured reflection coefficients for the design examples are shown in fig. 10. The measured and simulated findings are in good agreement.

TABLE II. Physical dimensions of prototype matching networks

Tx-lines	Example-1		Example-2	
	$Z(\Omega); \theta(deg)$	W/L (mm)	$Z(\Omega); \theta(deg)$	W/L (mm)
TL1	57.42;69.23	0.92/35.7	32.1;27.27	2.22/13.6
TL2	70.6;69.23	0.65/36	52.5;27.27	1.08/14
Tstub	81.56;69.23 (openstub)	0.44/36.7	51;27.27 (shortstub)	1.1/13.9
TLT	34.5;57.87	2/28.7	73.3;37.3	0.58/19.6
TLX	60;25	0.85/12.9	30;10	2.44/4.9

**Fig.9. Fabricated structures for the prototype matching networks.****Fig.10. Simulated and measured results for DBMNs for (a) Example-1, and (b) Example-2.**

4. CONCLUSION

A novel concept of concurrent dual band complex to real matching network using load shifters has been introduced in this paper. The limitations of a single section transmission line used for FDCL to CCL transformation which is used in several earlier proposed DBMNs has been discussed. Also, the possible range of loads at one frequency if the load at other frequency is given is thoroughly studied. It has been established through several examples that an otherwise unachievable FDCL to CCL transformation can easily be realized by integrating load shifters. The offered scheme is applied to design two prototype MNs at low ($m= 1.6$) and high ($m= 5.6$) frequency ratios. The proposed scheme is generic in nature and could be applied in all other conventional complex to real impedance matching networks as well.

REFERENCES

1. D. M. Pozar, *Microwave engineering*. John Wiley & sons, 2011.
2. C. Monzon, "A small dual-frequency transformer in two sections," *IEEE Transactions on Microwave Theory and Techniques*, vol. 51, no. 4, pp. 1157–1161, 2003.
3. M.-L. Chuang, "Analytical design of dual-band impedancetransformer with additional transmission zero," *IET Microwaves, Antennas and Propagation*, vol. 8, no. 13, pp. 1120–1126, 2014.
4. S. Rabbani, S. Narayana, and Y. K. Singh, "Enhancing loadrange of concurrent dual-band real to real

- matching network using load shifters,” in *2022 IEEE Microwaves, Antennas, and Propagation Conference (MAPCON)*. IEEE, 2022, pp. 316–321.
5. M.A. Maktoomi, R.Gupta, and M.S.Hashmi, “A dual-band impedance transformer for frequency-dependent complex loads incorporating an l-type network,” in *2015 Asia-Pacific Microwave Conference (APMC)*, vol. 1, 2015, pp. 1–3.
6. J. Liu, X.Y. Zhang, and C.L. Yang, “Analysis and design of dual-band rectifier using novel matching network,” *IEEE Transactions on Circuits and Systems II: Express Briefs*, vol. 65, no. 4, pp. 431–435, 2018.
7. S. Muhammad, J.J. Tiang, S.K. Wong, A. Smida, R. Ghayoula, and A. Iqbal, “A dual-band ambient energy harvesting rectenna design for wireless power communications,” *IEEE Access*, vol. 9, pp. 99944–99953, 2021.
8. X. Gui, C. Yu, S. Li, M. Su, and Y. Liu, “Design of dual-band power amplifier based on band-stop input matching structure,” in *2021 IEEE Asia-Pacific Microwave Conference (APMC)*, 2021, pp. 488–490.
9. M. Nikravan and Z. Atlasbaf, “T-section dual-band impedance transformer for frequency-dependent complex impedance loads,” *IET Electron. Lett.*, vol. 47, no. 9, pp. 551–553, 2011.
10. S. L. C. Y. Y. Wu, Y. Liu, “New coupled-line dual-band dc-block transformer for arbitrary complex frequency-dependent load impedance,” *Wiley Microw. and Opt. Tech. Lett.*, vol. 54, no. 1, pp. 139–142, 2012.
11. F.M. Ghannouchi, Mohammad A. Maktoomi, Mohammad S. Hashmi, “At-section dual-band matching network for frequency-dependent complex loads incorporating coupled line with dc-block property suitable for dual-band transistor amplifiers,” *Progress In Electromagnetics Research C*, vol. 54, pp. 75–84, 2014.
12. M. A. Maktoomi, M. S. Hashmi, and V. Panwar, “A dual-frequency matching network for fdcls using dual-band $\lambda/4$ -lines,” *Progress In Electromagnetics Research Letters*, vol. 52, pp. 23–30, 2015.
13. S. Rabbani, S. Narayana, and Y. K. Singh, “A novel concurrent dual band matching network for complex to real impedance matching for rf applications,” *IEEE Transactions on Circuits and Systems II: Express Briefs*, vol. 70, no. 1, pp. 66–70, 2023.
14. M. A. Maktoomi, M. S. Hashmi, and F. M. Ghannouchi, “Improving load range of dual-band impedance matching networks using load-healing concept,” *IEEE Transactions on Circuits and Systems II: Express Briefs*, vol. 64, no. 2, pp. 126–130, 2016.
15. M. Steer, *Microwave and RF Design*. Sci Tech Publishing, 2009.